UNITED STATES
NAVAL POSTGRADUATE SCHOOL

A STUDY OF THE ANTICLASTIC BENDING IN ELASTIC PLATES AND BARS

... *By* ...

GEORGE H. LEE
Professor of Mechanical Engineering

and

IVAR H. STOCKEL
Instructor of Mechanical Engineering

A Report
to the Office of Naval Research
upon an investigation conducted under
ONR Project Order No. NR-064-222

June 29, 1951

~~Engineering Division~~
Technical Report No. 3

U. S. Naval Academy Press—11-29-51—97

A STUDY OF THE ANTICLASTIC BENDING IN ELASTIC PLATES AND BARS

by

George H. Lee
Professor of Mechanical Engineering

and

Ivar H. Stockel
Instructor

United States Naval Postgraduate School
Annapolis, Md.

PREFACE

The Office of Naval Research Project, Number NR-064-22, for the study of the anticlastic bending in elastic plates and bars, was awarded the United States Naval Postgraduate School on 15 June 1950. The resignation of the present writer from the staff of the United States Naval Postgraduate School has made necessary the termination of this project after only one year. This report, then, presents the progress of the work during the period from 15 June 1950 to 29 June 1951. The work is incomplete but the results thus far obtained are of sufficient interest to be presented in the form of a report.

The authors wish to express their gratitude to the Office of Naval Research for sponsoring this project. The authors are also indebted to Captain H. T. Walsh, Assistant Superintendent, and to Dean R. S. Glasgow for making available the laboratory and shop facilities of the United States Naval Postgraduate School.

INTRODUCTION

Anticlastic bending is a phenomenon that occurs in varying degrees during the transverse bending of plates and bars. The origin of anticlastic bending is in the Poisson effect. For limited bending, i.e. if the curvature assumed by the plate or bar during bending is vanishingly small, anticlastic bending is assumed to occur. For other than vanishingly small curvatures in pure bending, anticlastic bending is assumed to occur if the plate or bar under consideration is "thick"; anticlastic bending is assumed to be restrained if the plate under consideration is "thin". The assumption of either free or restrained anticlastic bending is based on a rather nebulous differentiation between a "thick" and a "thin" plate.

Between the two limits, i.e. between entirely free and completely restrained anticlastic bending, there is a transitional range or region, in which the anticlastic bending is only partially restrained. The flexural rigidity of a plate in free anticlastic bending is well known. The flexural rigidity of a plate in restrained anticlastic bending is also well known. The flexural rigidity of a plate in partially restrained anticlastic bending, however, is not known. The behavior of the plate under partially restrained anticlastic bending, the stress condition at boundaries and the effect

of passing from free to restrained anticlastic bending are not known. Not only has this transitional range between free and restrained anticlastic bending not been studied, but there has been no specification of the limits for the transitional range.

It was the purpose of this investigation to carry out, concurrently, a theoretical and an experimental study of the transition range in anticlastic bending for elastic plates and bars. The effect of plastic deformation on the anticlastic bending was not to be considered in this study. The first approach to a theoretical solution of the problem is contained in this report. The theory presented is only approximate but the indications are that it yields results well within expectations. In fact, the classically assumed shape of a "thin" plate in completely restrained anticlastic bending is predicted by the theory presented. The experimental results are very limited due to the rather unexpected and early termination of the project. The instrumentation has been designed and constructed. Tentative observations have been made, checking the design and the construction. If data are available before this report is submitted, they will be attached as an appendix.

TABLE OF CONTENTS

I. THEORETICAL CONSIDERATIONS

I.1 Statement of the Problem

It is the purpose of this investigation to more completely describe the mechanism of the deformation of structural members in bending. This first analysis is concerned only with elastic plates and bars of rectangular cross-section, loaded in pure bending parallel to one of the two principal axes of the cross-section. Throughout the analysis, the structural material is assumed to be the idealized material with which the classical theory of elasticity is concerned.

In the classical derivations of the equations of equilibrium and compatibility and again in the applications of these equations, there is one basic assumption. This basic assumption is that the deformations occuring in the deformed structural member are such that neither the boundary conditions nor the state of stress are affected by the deformations.(1) This assumption has been employed to solve the problem of a beam in pure bending.(2) The deformed shape of the beam given by this solution is shown, exaggeratedly in figure (1).

---

(1) Timoshenko, S., Theory of Elasticity, 1st Ed., p. 202, McGraw-Hill Book Company, Inc., (1934)

(2) Timoshenko, S., op.cit., pp. 221-226

The longitudinal axis of the beam, which was coincident with the z-axis in the unstressed state, is now bent to a radius of curvature, R, given as:

$$R = EI/M$$

Here, E is Young's modulus of elasticity, I is the second moment of the cross-sectional area, assumed rectangular, with respect to the gravity axis parallel to the axis of bending, and M is the applied bending moment.

Although not considered in the solution of the above mentioned problem, the transverse axis of the beam which was coincident with the y-axis before bending is now bent to a radius of curvature R/μ, in which μ is Poisson's ratio. All lines which were parallel to the longitudinal and transverse axes of the beam, respectively, remain parallel to these axes although in the deformed state, they are curved. The sides of the beam section which were straight and vertical remain straight but become inclined symmetrically. The problem is symmetrical about any cross-section; hence any cross-section and therefore all cross-sections must remain plane.

Cursory experimental analyses of beams of nearly square cross-section have indicated that this solution is correct. In fact, the anticlastic shape of

beams has been used to determine Poisson's ratio.[3] As opposed to the agreement between theory and experiment for beams of nearly square cross-sectional area, plates (beams having large width to thickness ratios) subjected to pure bending in one dimension do not assume the shape predicted and observed in the above problem. Actually, no experimental investigation is known(by the present writers) to have been made on the true shape assumed by a plate in pure bending. Most workers in the field assume that the cross-sections of these plates remain rectangular. It has been the practice, in applications of the thin plate theory, to attribute the configuration assumed for thin plates to a moment distribution applied parallel to the z-axis.[4]

This difference in behavior between the thick beam and the thin plate subjected to pure bending must stem from the assumption that the equations of equilibrium and conpatibility are derived for, and the boundary conditions applied to, the unstressed geometry of the elastic beam or plate, since no other assumption has been allowed. It is, then, the task of this project to formulate and to establish methods of analysis of beams and plates in pure bending which

---

(3) Timoshenko, S., op.cit., p. 225

(4) Timoshenko, S., op.cit., p. 227

reduce the aforementioned difference to a minimum. Ideally, a derivation of the exact equations of equilibrium and compatibility and the exact expressions of the boundary conditions is desired. Such a derivation could possibly be made; the resulting equations, however, could not, currently, be solved for the general case. Several alternatives suggest themselves. The alternative chosen is to partially correct the solutions made from the existing theory by attempting to compensate for particular inconsistancies which become apparent in specific problems.

I.2 A Method of Analysis[5]

Consider the beam solution which was discussed in the preceeding section. It is proposed to analyze that solution and to attempt to correct the individual faults which may become apparent as a result of the present analysis.

The results of the previous problem are given as:

$$\sigma_z = \frac{Ex}{R}\,;\quad \sigma_x = \sigma_y = \tau_{xy} = \tau_{yz} = \tau_{zx} = 0$$

Thus, any longitudinal fiber may be regarded independently as a member in simple tension or simple compression. This combination of tension in some fibers and compression in others, accompanied by the Poisson contraction and expansion (figure 2) accounts for the anticlastic shape of the deformed beam. If the bending of the beam is other than vanishingly small, these tensions and compressions will have radial components, perpendicular to the principal axis of curvature. These radial components are not recognized to exist in

---

(5) A detailed derivation of this method of analysis is given in appendix I.

the classical solutions.[6] It is well to examine the alteration in the deformation of the beam which follows from the action of them.

Refer to figure 4. The cross-sectional shape of the beam shown is that which is produced by completely "free" anticlastic bending; i.e. by denying the presence of any stress component which is not parallel to the z-axis. The neutral surface of the plate or beam must become cylindrical as bending occurs; hence it can no longer coincide with the midsurface of the beam. Although the beam is bent to a curvature 1/R, it will be assumed that the straight beam theory holds.[7] Thus the stress varies directly as the distance from the neutral surface. It is seen from figure 4, then, that there are more fibers in compression than in tension in the midportion of the beam and that there are more fibers in tension than in compression in the side portions of the beam.

Now, account is taken for the radial components of σ_z. From the anti-symmetry of σ_z with respect to the neutral surface (figure 4) there follows the anti-symmetry of the radial components of σ_z. We will call these radial components σ_r', figure 5. More descriptively, there are, in the center of the beam, more

---

(6) Timoshenko, S., op.cit. pp. 221-227

(7) This assumption introduces a maximum error of 0.66%. This error is calculated in Appendix 1.

fibers which exert radial components of greater magnitudes away from the principal axis of curvature than towards it, and there are, in the side portions of the beam, more fibers which exert radial components of greater magnitudes towards the principal axis of curvature than away from it. Such an unbalance of those components would seem to tend to reduce the anticlastic curvature of the beam. Specifically, the aim of this analysis is to determine the distortion of the free anticlastic shape produced by considering these radial components.

Imagine a portion of the beam of figure 5 between two cross-sections separated by a unit arc at the neutral surface to be another beam, figure 6. Ideally, the radial component of σ_z, i.e. σ_n', of figure 5, may be thought of as a body force which varies in proportion to the distance from the neutral surface. However, it is important to understand that because the body force at any point in the beam is a function of the position of that point and because these positions are changed by the action of them, the body forces vary under their own actions. Thus a method of solution is proposed.

1. Bend a rectangular sectioned beam to a principal radius of curvature $\underline{R}$, and specify that no radial component of stress shall exist (elementary theory).

2. Determine the cylindrical neutral surface by stating that the longetudinal stresses vary linearly from it and that their integral over a section is zero.

3. Consider a section of the beam between two cross-sections separated by a unit arc at the neutral surface to be an isolated elastic body.

4. Allow the actions of the radial components in the slab to exist (as body forces), but deny the actions of the longitudinal stresses.(8)

5. The principal radius of curvature is to be fixed, i.e. the neutral surface of the beam is to be cylindrical in shape and of fixed radius, R.

6. Due to the specifications, the problem assumes a radial symmetry with respect to the principal axis of curvature. We may now mathematically express the radial components of the stress in the fibers as a linear function of the displacement of the fibers relative to the neutral surface. Thus these components vary only as a result of the relative motion of their fibers with respect to the neutral surface and not as a result of a change in the apparent stiffness of the original beam since R is maintained constant.

7. Include these body forces in the equations of

---

(8) See Appendix 1.

equilibrium and take all body forces to be zero.

The beam which has been described, figure 6, would be a difficult one to study mathematically. The problem can be greatly simplified with the introduction of a small error; (a) by assuming that σ_r' acts through the center of anticlastic curvature and (b) by summing the body forces of figure 6 in that direction and thus by applying them as an edge loading, figure 7.[9] Of course, this edge loading must vary under its own application. This variation in the edge loading can be handled with relative ease by introducing a change in variables. Thus the problem illustrated in figure 7 is altered to the problem illustrated in figure 8. The deflection curve found for the beam of figure 8 will be realtered to correct for this change. The problem of figure 8 is precisely that of a beam on an elastic foundation subject to a prescribed loading. That is to say that the elastic foundation acts to compensate for the necessary variation in the edge loading.

The solution for this problem is indicated in Appendix 1. The final result is given here as:

$$y_3' = D\cos\frac{\mu}{R}x' + E\left[F\cosh\beta x'\sin\beta x' + G\sinh\beta x'\cos\beta x'\right] \qquad (22)$$

---

(9) Timoshenko, S., op.cit., p. 87. Along with this simplification, it willbe assumed that only the deflection of the mid-surface of the beam in figure 7 is sought and that the thickness of the beam in the radial direction does not vary.

The constants are found to have the values:

$$D = \frac{a^2 R \mu^3}{a^2 \mu^4 + 3R^3(1-\mu^2)} \tag{23}$$

$$E = \frac{\sqrt{2a^3R^5\mu}\left[3(1-\mu^2)\right]^{1/4}}{\left[a^2\mu^2+3R^3(1-\mu^2)\right]\left[\sin\beta b\cos\beta b+\sinh\beta b\cosh\beta b\right]} \tag{24}$$

$$F = \beta\cos\frac{\mu}{R}b\left[\sinh\beta b\cos\beta b - \cosh\beta b\sin\beta b\right] + \\ + \frac{\mu}{R}\sin\frac{\mu}{R}b\cosh\beta b\cos\beta b \tag{25}$$

$$G = \beta\cos\frac{\mu}{R}b\left[\sinh\beta b\cos\beta b + \cosh\beta b\sin\beta b\right] + \\ + \frac{\mu}{R}\sin\frac{\mu}{R}b\sinh\beta b\sin\beta b \tag{26}$$

I.3 Results of this Analysis

Equation (22) of the previous section is sufficiently complex in form to require a visual analysis of its graphs for a number of specific cases. The parameters which may vary to specify a particular problem are: μ, Poisson's ratio; R, radius of curvature of the neutral surface; a, half height of beam; b, half width of beam. Poisson's ratio varies only slightly, between 1/4 and 1/3, for most structural materials. Hence, it is given the value of 1/4 for all computations. Of the three remaining parameters, a, b and R, one may be fixed since it is reasonable to assume that some form of geometric similitude must exist in the problem. Therefore, b is set equal to 10. The following two families of cases are solved. In the first case,

a is varied:

a = 2, 1, 1/2, 1/10, 1/100
R = 20
b = 10
μ = 1/4

and in the second case, R is varied:

R = 20, 50, 100
a = 1
b = 10
μ = 1/4

Figures 9 and 10 are graphs of the former and latter families, respectively. In each case the transverse curve of the mid-surface for completely free anticlastic bending is included in dashed lines. From a study of these graphs, the following conclusions may be drawn.

1. There exist two ranges of restrained anticlastic bending.

   a. One range in which the radius of anticlastic curvature is increased and becomes variable over the width of the plate. Bending in this range will be termed partially restrained anticlastic bending.

   b. The second range is one in which there no longer exists any semblence of the original anticlastic curvature. In this range, the transverse curve of the midsurface appears to assume a sinusoidal form of exponentially increasing

amplitude as the edge of the plate is approached. Bending in this range shall be termed restrained anticlastic bending.

2. In the first family, the boundary between partially restrained and restrained anticlastic bending lies in the interval that separates the cases $a = 1$ and $a = 1/2$, for $R = 20$

3. In the second family, the boundary between nearly free and partially restrained anticlastic bending lies near the case $R = 100$, $a = 1$.

4. The degree of restraint is very possibly an inverse function of a and R.

Since the expression for the deflection of the midsurface is sinusoidal the question arises whether or not the edges of the midsurface will in any case of restrained anticlastic bending have negative deflection, i.e. will the edge of the midsurface lie on the same side of the neutral surface as the principal axis of curvature. Equation (22) has been solved in Appendix II for the deflection of the edges for the general case. It is proven there that the edges of the midsurface will never, for any degree of pure bending of the beam, have a negative deflection. Physically, this would be expected; this proof was to check the mathematical solution.

The foregoing conclusions suggest that the boundary between free and partially restrained anticlastic bending may be investigated by merely solving for the deflection of the midsurface at its center line. For convenience of analysis, the degree of partially restrained anticlastic bending is defined as: 100 times the ratio of the difference between the deflections of the midsurface at their centers of the completely free and the partially restrained curves to the deflection of the completely free curve. From figure 10, we have:

$$\psi = \frac{f-s}{f} 100$$

The parameter ψ was calculated for the following cases ($\mu = 1/4$, $\underline{b} = 10$):

a	R	ψ
1	50	28
1	100	7
1	500	1
1	1000	0
1/10	50	-
1/10	100	-
1/10	500	28

a	R	ψ
1/10	1000	7
1/10	5000	1
1/10	10000	0
1/100	5000	28
1/100	10000	7
1/100	50000	1
1/100	100000	0

From this table of values and from conclusion (4) above, it would seem that ψ is an inverse function of the product $\underline{aR}$. It will be remembered that $\underline{b}$ has been held constant in all cases. On the basis of geometrical similarity, then, one might conclude that ψ is a function of the dimensionless parameter b^2/aR. Reference to equation (22) will indicate that the quantity

β b may be written in the form:

$$\beta b = \left[\frac{3(1-\mu^2)}{4a^2R^2}\right]^{1/4} b = K\sqrt{b^2/aR}$$

Thus ψ might as well be written as a function of b.

In the light of these indications and also because of the values found in the computations for other terms, equation (22) can be more intelligently analyzed.

In all the computations, the term

$$-D\cos\frac{\mu}{R}x'$$

is small, and its variation smaller, compared to the deflection. Hence, it may be dropped. Furthermore, the coefficient, E, may be simplified as:

$$E' = \frac{\mu a\sqrt{2Ra}}{\left[3(1-\mu^2)\right]^{3/4}\left[\cos\beta b\sin\beta b + \cosh\beta b\sinh\beta b\right]}$$

It can be shown in all the computations, that the second terms of the expressions for both F and G may be neglected for all cases of partially restrained bending and for those cases of restrained bending which lie near the range of partially restrained beinding. This is not true for some cases in which the beam is bent well within the restrained range. Thus equation (22) may be approximated by:

$$y_d' = E'\left(F\cosh\beta x'\cos\beta x' + G\sinh\beta x'\sin\beta x'\right)$$

and, with the exception of some cases which lie well within the restrained range:

$$y_d' = \frac{a\mu}{\sqrt{3(1-\mu^2)}}\left[\frac{\sinh\beta b\cos\beta b - \cosh\beta b\sin\beta b}{\sin\beta b\cos\beta b + \sinh\beta b\cosh\beta b}\cos\beta x'\cosh\beta x' + \right.$$

$$\left. + \frac{\sinh\beta b\cos\beta b + \cosh\beta b\sin\beta b}{\sin\beta b\cos\beta b + \sinh\beta b\cosh\beta b}\sin\beta x'\sinh\beta x'\right]$$

From the foregoing equation it becomes clear that the form of y_d' depends entirely upon βb and, consequently, upon b^2/aR. Thus on the basis of the table for ψ, a and R given above the indication that ψ is a function of βb alone, the graph in figure 11 is plotted.

I.4 Conclusions and Discussion of Results

According to the analysis made in the preceding sections, the manner in which prismatic bars are deformed in pure bending may be separated into three classifications, depending upon the value of the parameter b^2/aR where a is less that R/100, see figure 11.(10)

1. Completely free anticlastic bending, $b^2/aR < 1/5$.
   In this range the deformed shape of the beam is within 1% of the shape found by the application of the elementary theory.(11)
2. Partially restrained anticlastic bending, $1/5 < b^2/aR < 7.5$

---

(10) See Appendix I

(11) Timoshenko, S., op. cit. pp. 221-227

In this range, the deformed shape of the beam resembles the free anticlastic bending shape. However, the anticlastic radius of curvature has been increased and becomes variable over the width of the beam. The value of R, here denoted by R', may be approximated by the relation:

$$R' = \frac{R}{\mu} \frac{1}{1 - \Psi/100}$$

where Ψ is taken from the graph in figure 11.(12)

3. Restrained anticlastic bending, $7.5 < b^2/aR$.

In this range, the deformed shape of the beam no longer resembles the free anticlastic shape. The midsurface becomes corrugated; the amplitudes of the corrugations grow almost exponentially as the edge of the beam is approached, see figure 9. It is seen that only the last negative and positive sweeps of these corrugations are apparent and that the center of the beam is essentially flat (to within 0.1 microinches).

This analysis has been an attempt to closely approximate the truth. The reasonability of many of the assumptions, which have been made here, is difficult to judge. Hence, the experimental phase of this investigation is left with the task of appraising the work. Should experimental data not agree with the present solution, there are opportunities in the theoretical approach for further corrections or modifications.

---

(12) See Appendix II

II EXPERIMENTAL APPROACH

II.1 Required Analysis

The results of the theoretical analysis which were presented in the previous sections must be compared with experimental data to establish their validity. It is proposed, here, to explore by experimental methods, the limits established by theory for the transitional range in anticlastic bending. With this in mind, test specimen were chosen to closely follow those suggested in section I.4.

Instruments have been designed and constructed to supply the necessary data. It is the object of the following paragraphs to briefly describe these instruments.

II.2 Beam Specimen

The Brown and Sharpe Company of Providence, R.I. produce a flat ground stock of first quality tool steel in sizes which cover the desired range of size very nicely. The previous results suggest that the range of specimen size $4 < b/a < 100$ be chosen. Twelve thicknesses of stock, all 1 1/2" wide were obtained that covered this range.

+The methods for exploring the contours of the bent specimen are such that the test surface must be smooth and flat. Accordingly, a lapping machine was designed and constructed. This lapping machine is of sufficient

size to prepare a test area of 1 1/2" (the width of the specimen) by 2". The contours to be explored must be sufficient to determine the principal radius of curvature and the transverse curvature.

II.3 Method of Loading Specimen

It is desired to load the specimen in pure bending. A test jig has been constructed and checked. Tuckerman strain gages were used on a trial specimen in the test jig and, within the limitations of the strain gages, the test specimen was found to be in pure bending. The test jig is somewhat along standard lines. The only modification incorporated is a worm-gear combination designed to maintain the lever arms horizontal regardless of the curvature assumed by the test specimen.

II.4 Contour Measurement by a Light Interference Method

The first method to be employed in measuring the contours of the bent beam is a standard, reflection, interference method. The interference fringes will be recorded photographically. Since this is a well known method, no more will be said concerning it.

There is, however, one serious difficulty encountered in the application of this method. The contours of the beam specimen must be determined before loading is applied and again at successive increments of loading. It is planned to rest the optical flat on the beam. As the beam is bent, extreme care must be taken to maintain

the proper orientation of the optical flat. As this method is applied, it may become necessary to support the optical flat in a manner independent of the beam.

II.5 Contour Measurement by a Pneumatic Micrometer

Within relatively recent years, a pneumetic micrometer has been developed[13] and applied as the amplification element in strain gages, inspection gages, flattness gages, etc. The magnification and sensitivity are both very high and the calibration of the system is quite stable. A contour measuring device has been designed employing this principle. This device has not as yet, been checked out but every confidence is placed in its ability to meet the needs of this investigation.

An interferometer calibration device has also been constructed for the calibration of the pneumatic device. Several novel modifications have been incorporated in this calibration device; aside from these modifications, however, it is along standard lines.

---

(13) WILDHACK, W.A., Versatile Pneumatic Instrument Based on Critical Flow, Rev.Sci.Instr., 21, 25-30 (1930)
de LEIRIS, H., Sur la Mesure des Constantes Elastiques par Amplification Pneumatique des Deformations, 5th Intern.Cong.Appl.Mech.,Proc. (1939)
DUMANOIS,WATTEBOT,OUTIN,deLEIRIS,BENSIMON and NICOLAU, La Metrologie Pneumatique, Mecanique, 69-83 (Mar-Apr 1937)
de LEIRIS, H., Sur une Nouvelle Methode d'Amplification Pneumetique et ses Amplification en Extensometrique, 7th Intern.Cong.Appl.Mech., Proc. 121-127 (1948)
RAUM,M., Das Pneumatische Prüfverfahren, Zeits.f. Techn,Phys., no. 3, 46-53 (1943)

APPENDIX I

DETAILED DERIVATION OF A METHOD OF THEORETICAL ANALYSIS

We will consider a long beam, illustrated in figures 1 and 1a, whose z-axis has been bent in completely free anticlastic bending to a principal radius of curvature of R. We wish to determine the normal stresses parallel to the z axis as functions of r and θ. All letters and symbols that are not shown in the figures are defined as they are introduced.

We assume that plane cross-sections remain plane after bending. Therefore:

$$\sigma_z = J(x - e) \qquad (1)$$

where σ_z is the normal stress and J is a constant of proportionality. We have, here:

$$x = \frac{R}{\mu} - x'' \qquad \text{and} \qquad x'' = r\cos\theta$$

Then:

$$\sigma_z = J\left(\frac{R}{\mu} - e - r\cos\theta\right) \qquad (2)$$

Since the beam is in pure bending, we may write one of the boundary conditions as:

$$\int_A \sigma_z \, dA = 0$$

or

$$J = \int_0^{\Phi} \int_{\frac{R}{\mu}-a}^{\frac{R}{\mu}+a} \left(\frac{R}{\mu} - e - r\cos\theta\right) r\, dr\, d\theta$$

where A is the cross-sectional area. From the above, then, we may write:

$$e = \frac{R}{\mu} - \frac{1}{36}\left(3\frac{R^2}{\mu^2} + a^2\right)\sin\frac{b\mu}{R} \qquad (3)$$

The second moment of the cross-sectional area, with respect to the neutral axis, is defined as:

$$I_e = \int_A (x-e)^2\, dA$$

and the bending moment may be written as:

$$M = \int_A (x-e)\sigma_z\, dA$$

From these two equations, and employing equation (1), we have:

$$I_e = \frac{M}{J}$$

Since, from the elementary beam theory:

$$\frac{1}{R} = \frac{M}{EI_e} \qquad \text{or} \qquad M = \frac{EI_e}{R}$$

We then have:

$$J = \frac{E}{R} \qquad (4)$$

The normal stress, σ_z , may now be written as:

$$\sigma_z = \frac{E}{R}\left[\frac{1}{3b}\left(3\frac{R^2}{\mu^2}+a^2\right)\sin\frac{b\mu}{R} - r\cos\theta\right]$$

We will substitute

$$B' = \frac{1}{3b}\left(3\frac{R^2}{\mu^2}+a^2\right)\sin\frac{b\mu}{R}$$

The normal stress is now written as:

$$\sigma_z = \frac{E}{R}\left(B' - r\cos\theta\right) \qquad (5)$$

Refer to figure 3a. The radial component of the normal stress, indicated as σ_r', is written, for the differential element shwon, as:

$$\sigma_r' = 2\left(\sigma_z\right)\left(\frac{\Delta\alpha}{2}\right)\Big/\Delta z = 2\sigma_z\,\frac{\Delta\frac{z}{R}}{\Delta z} = \frac{\sigma_z}{R} \qquad (6)$$

The resolution of the stresses is illustrated in figure 6. Consider the slab shown as an isolated elastic body. The radial components of σ_z , i.e. σ_r' , are seen to act as "body forces". It will be noted that along any given principal radial ordinate, these stresses are not necessarily balanced. Consequently, these "body forces" are thought to be "responsible", at least in part, for the partial and complete restraint of anticlastic bending of bars and plates. If this latter is true, it seems reasonable that the deflection shape of the

slab shown, under the action of these body forces, will be that of the final transverse shape assumed by the actual beam. It must be remembered, however, that these body forces are dependent upon the deflection shape and, therefore, must be introduced as functions of that shape.

The solution of the beam problem described above is a difficult one. Consequently, the beam is simplified to the one shown in figure 8 by (a) assuming the resultants act through the anticlastic center of curvature, (b) integrating the body forces across the beam in the radial direction (anticlastic) and by representing these body forces as an edge loading, (c) straightening the beam, thus making the mid-plane (R = constant) be along the x-axis, and (d) compensating for the variation in edge loading, as a function of the deflection shape, by placing the beam on an elastic foundation.

Accordingly, the edge loading, $L(\theta)$, is written:

$$L(\theta) = \int_{\frac{R}{\mu}-a}^{\frac{R}{\mu}+a} \sigma_x' \, dn = \int_{\frac{R}{\mu}-a}^{\frac{R}{\mu}+a} \frac{\sigma_x}{R} \, dn$$

$$= \frac{2aE}{R^2}\left(\delta' - \frac{R}{\mu}\cos\theta\right)$$

Transfer of the coordinate system of figure 8 yields:

$$\theta = \frac{\mu}{R}x' \qquad (8)$$

We may then write:

$$L(x') = \frac{2aE}{\mu R}\left(B - \cos\frac{\mu}{R}x'\right) \qquad (9)$$

where

$$B = \frac{\mu}{3Rb}\left(3\frac{R^2}{\mu^2} + a^2\right)\sin\frac{b\mu}{R} \qquad (10)$$

The differential equation for a beam loaded on an elastic foundation is written as:

$$(EI_e)'\frac{d^4y'}{dx'^4} - ky = L(x') \qquad (11)$$

where $(EI_e)'$ is the "plate" rigidity per unit width, or

$$(EI_e)' = \frac{8a^3E}{12(1-\mu^2)} = \frac{2a^3E}{3(1-\mu)} \qquad (12)$$

The plate rigidity has been used rather than the beam rigidity (EI) because the slab, as a result of actually being part of the original beam, is completely restrained in its transverse direction.

It is necessary to determine the value of k in equation (11). As stated above, the purpose of the elastic foundation is to account for the variation in σ_z and therefore L(x') as the beam is deflected by L(x'). A variation in y' of the coordinate system of figure 8 is analogous to a variation of x in the coordinate system of figure 6 (allowing simplification (c) stated above).

Since σ_x was given to vary directly with x, then L(x') varies directly with y'. Hence the constant k may be written:

$$k = \frac{d}{dx} L(x') \tag{13}$$

It has been allowed that

$$y = -(x_s - e)$$

here, x_s is the x coordinate of the mid-plane in figure 1a. Then:

$$y' = \frac{R}{\mu}(\cos\theta - B) \tag{14}$$

and

$$L(x') = -\frac{2aE}{R^2} y'$$

It follows, then, that:

$$k = -\frac{2aE}{R^2} \tag{15}$$

Equation (11) may then be written:

$$\frac{d^4y'}{dx'^4} + \frac{3(1-\mu^2)}{a^2R^2} y' = \frac{3(1-\mu^2)}{a^2\mu R}\left(B - \cos\frac{\mu}{R}x'\right) \tag{16}$$

let

$$\beta = \left(\frac{3(1-\mu^2)}{4a^2R^2}\right)^{1/4} \quad \& \quad C = \frac{3(1-\mu^2)}{a^2\mu R} \tag{17}$$

Equation (16) may now be written:

$$\frac{d^4y'}{dx'^4} + 4\beta^4 y' = C\left(B - \cos\frac{\mu}{R}x'\right) \tag{18}$$

The particular integral of equation (18) is:

$$y_p' = C\left(\frac{B}{4\beta^4} - \frac{\cos\frac{\mu}{R}x'}{\left(\frac{\mu}{R}\right)^4 + 4\beta^4}\right) \tag{19}$$

The complementary solution is:

$$y_c' = C_1 \cosh\beta x' \cos\beta x' + C_2 \sinh\beta x' \sin\beta x' + C_3 \cosh\beta x' \sin\beta x' + C_4 \sinh\beta x' \cos\beta x' \qquad (20)$$

We see that y'_c must be symmetrical with respect to the y'-axis and so C_3 and C_4 must be equal to zero. At the ends of the beam, the shear force and bending moment are both equal to zero. This yields:

$$\left(\frac{d^3y'}{dx'^3}\right)_{x'=\pm b} = \left(\frac{d^2y'}{dx'^2}\right)_{x=\pm b} = 0 \qquad (21)$$

where

$$y' = y_p' + y_c'$$

Thus C_1 and C_2 are determined and so y' is defined. It will be recalled, however, that the beam was not straight originally. Consequently, its original deflection must be subtracted from y' since it was, in effect, added when the beam was considered to have been straightened. Then:

$$y_d' = y' - y'_{(14)} = y_p' + y_c' - y'_{(14)}$$

where $y'_{(14)}$ is the value of y' from equation (14). From equations (8), (14), (17), (19) and (20), we have:

$$y_d' = -D\cos\frac{x'}{R} + E\left(F\cosh\beta x'\cos\beta x' + G\sinh\beta x'\sin\beta x'\right) \qquad (22)$$

where:

$$D = \frac{a^2 R \mu^3}{a^2\mu^4 + 3R^2(1-\mu^2)} \qquad (23)$$

$$E = \frac{\sqrt{2aR^5}\,\mu\,[3(1-\mu)]^{1/4}}{\left[a^2\mu^2 + 3R^2(1-\mu^2)\right]\left[\sin\beta b\cos\beta b + \sinh\beta b\cosh\beta b\right]} \qquad (24)$$

$$F = \beta\cos\frac{\mu}{R}b\left(\sinh\beta b\cos\beta b - \cosh\beta b\sin\beta b\right) + \\ + \frac{\mu}{R}\sin\frac{\mu}{R}b\cosh\beta b\cos\beta b \qquad (25)$$

$$G = \beta\cos\frac{\mu}{R}b\left(\sinh\beta b\cos\beta b + \cosh\beta b\sin\beta b\right) + \\ + \frac{\mu}{R}\sin\frac{\mu}{R}b\sinh\beta b\sin\beta b \qquad (26)$$

APPENDIX II

1. Consider the value of the constant E in equation (24). Since we have specified that a is less than R/100, the first and second terms in the first factor of the denominator of equation (24) may be compared.

$$\frac{a^2\mu^2}{3R^2(1-\mu^2)} = \frac{\mu^2}{30{,}000(1-\mu^2)} \approx 0.000002$$

Hence the first factor will be dropped and we have:

$$E' = \frac{\mu a\sqrt{2aR}}{[3(1-\mu^2)]^{3/4}[\cos\beta b \sinh\beta b + \cosh\beta b \sin\beta b]}$$

2. Consider the first terms in the constants F and G as compared to the first terms in these constants. It is specified that a be less than R/100 and that b^2/aR be less than 9. Then F may be written as:

$$F = \frac{9.16}{R}\cos\frac{b}{4R}\left[\sinh\frac{9.16b}{R}\cos\frac{9.16b}{R} - \cosh\frac{9.16b}{R}\sin\frac{9.16b}{R}\right] +$$

$$+ \frac{1}{4R}\sin\frac{b}{4R}\cosh\frac{9.16b}{R}\cos\frac{9.16b}{R}$$

where $b/r < 0.3$, from information given above. The terms shown in the brackets are of the same order of magnitude; this also applied to the constant G. Hence compare the maximum value of the coefficient of the second with the minimum value of the coefficient of the first:

Hence, in the [illegible]

$$y_d' = \frac{[illegible]}{[illegible]}\left[\frac{[illegible]}{[illegible]}\cosh\beta x \cos\beta x' + \right.$$

$$\left. + \frac{[illegible]}{[illegible]}\sinh\beta x' \sin\beta x'\right]$$

3. It is to be [illegible] is positive in all cases [illegible]

$$y'_{d(x'=\pm b)} = E\beta[illegible]\cosh\beta b\cos\beta b - \sin\beta b\cos\beta b] +$$

$$+ E\frac{\mu}{R}[illegible][\cosh^2\beta b \sin^2\beta b]$$

E in equation [illegible] positive for all values of b since the [illegible] functions is always equal to or [illegible] product of the trigonometric functions [illegible] first set of brackets in the equation [illegible] is always positive for the same [illegible] trigonometric functions of $\mu b/R$ will be [illegible] all values of $\mu b/R$ which lie within the range [illegible] applied. The term in the second [illegible] is always positive because all factors [illegible] hence the value of y' at $x = \pm b$ is positive [illegible] within the range considered.

4. To determine the relationship:

$$R' = \frac{R}{\mu} \frac{1}{1 - \Psi/100}$$

We have defined the quantity Ψ as:

$$\frac{\Psi}{100} = \frac{f - s}{f}$$

but

$$f \approx \frac{R}{\mu}\left(\frac{R}{\mu b} \sin \frac{\mu b}{R} - 1\right)$$

from equations (10) and (14) where $a < R/100$. Expanding:

$$f \approx \frac{R}{\mu}\left[1 - \frac{\left(\frac{b\mu}{R}\right)^2}{6} - 1\right] = \frac{b^2\mu}{6R}$$

Assume the R' exists, then:

$$s \approx \frac{b^2}{6R}$$

Hence:

$$\frac{\Psi}{100} \approx \frac{\frac{b^2\mu}{6R} - \frac{b^2}{6R}}{\frac{b^2\mu}{6R}}$$

or

$$R' \approx \left(\frac{R}{\mu}\right) \frac{1}{1 - \Psi/100}$$

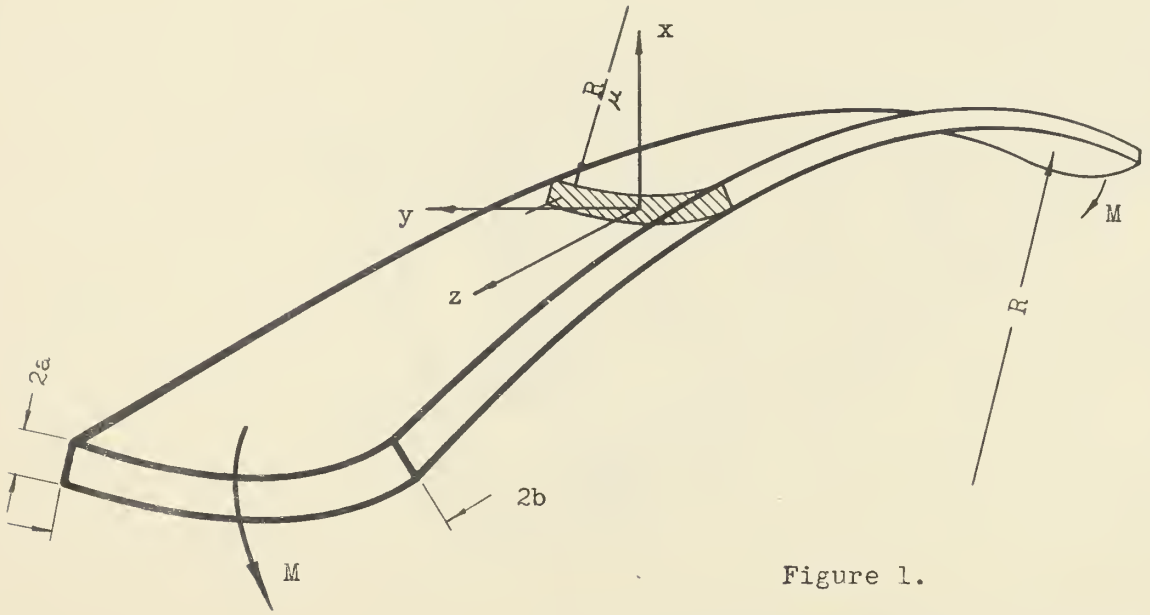

Figure 1.

Prismatic Bar Bent in Completely Free Anti-clastic Bending

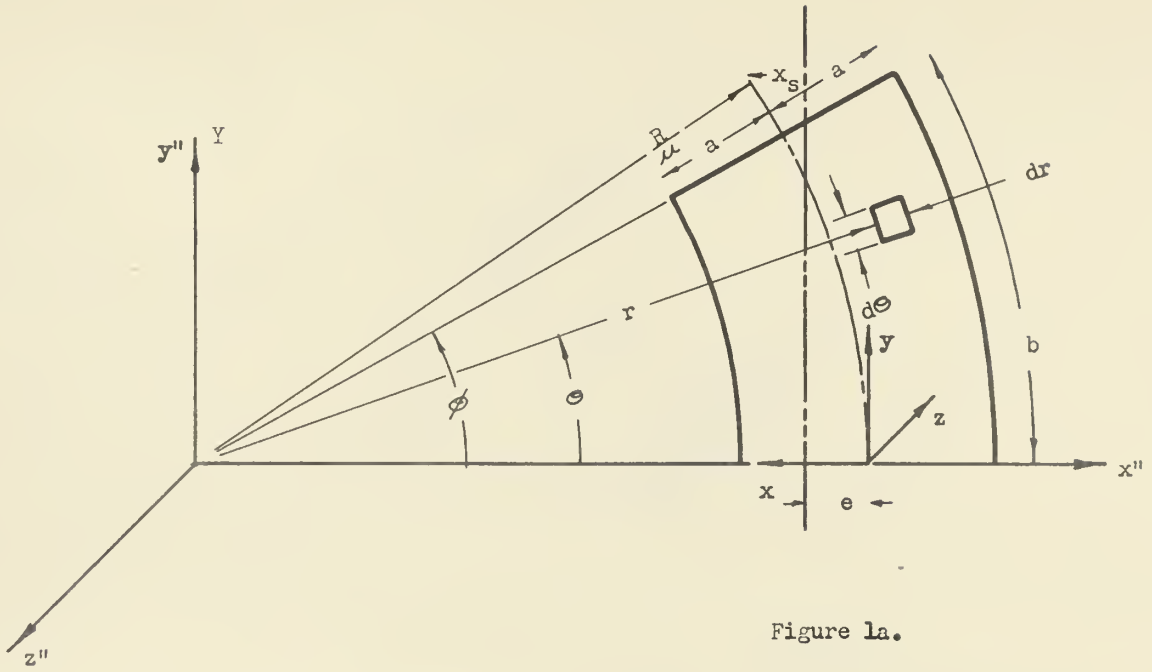

Figure 1a.

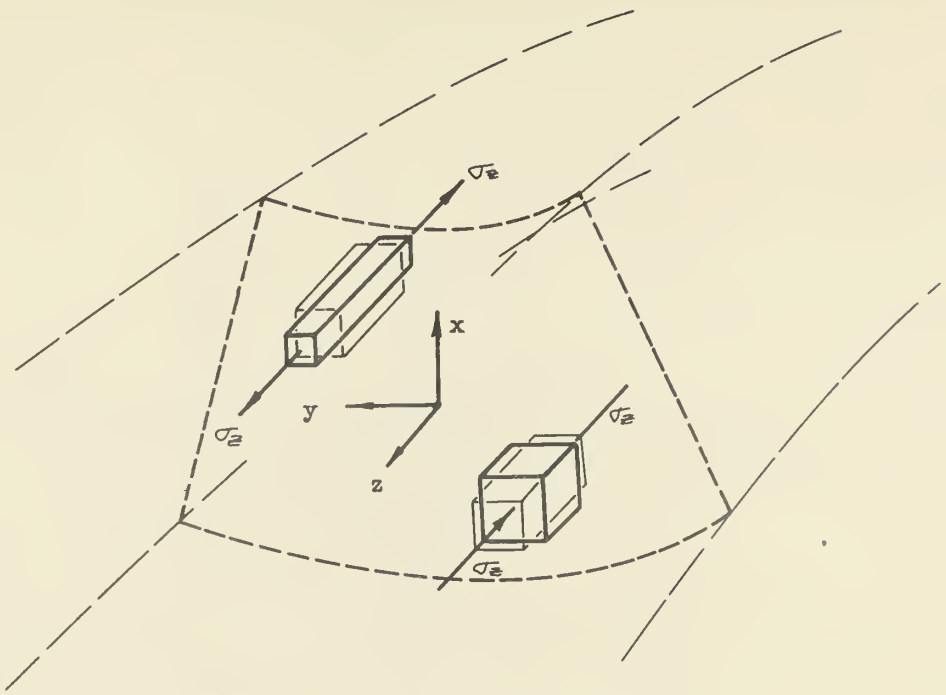

Figure 2,

Portion of Prismatic Bar Bent in

Completely Free Anti-clastic Bending

Showing Contraction and Expansion in the

x and y Directions

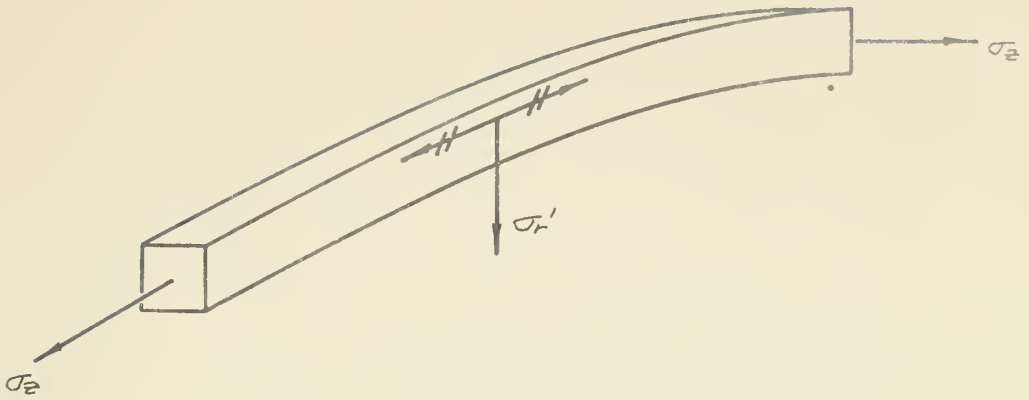

Figure 3.

Fiber Showing Resolution of Forces

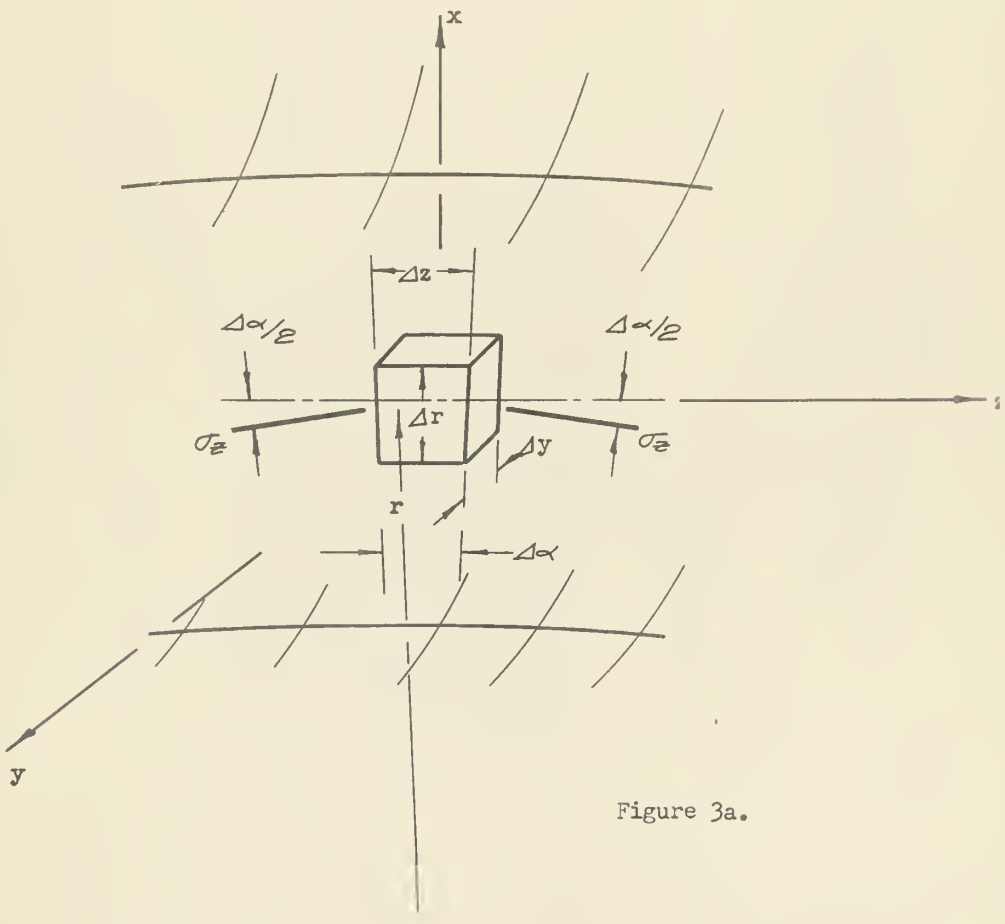

Figure 3a.

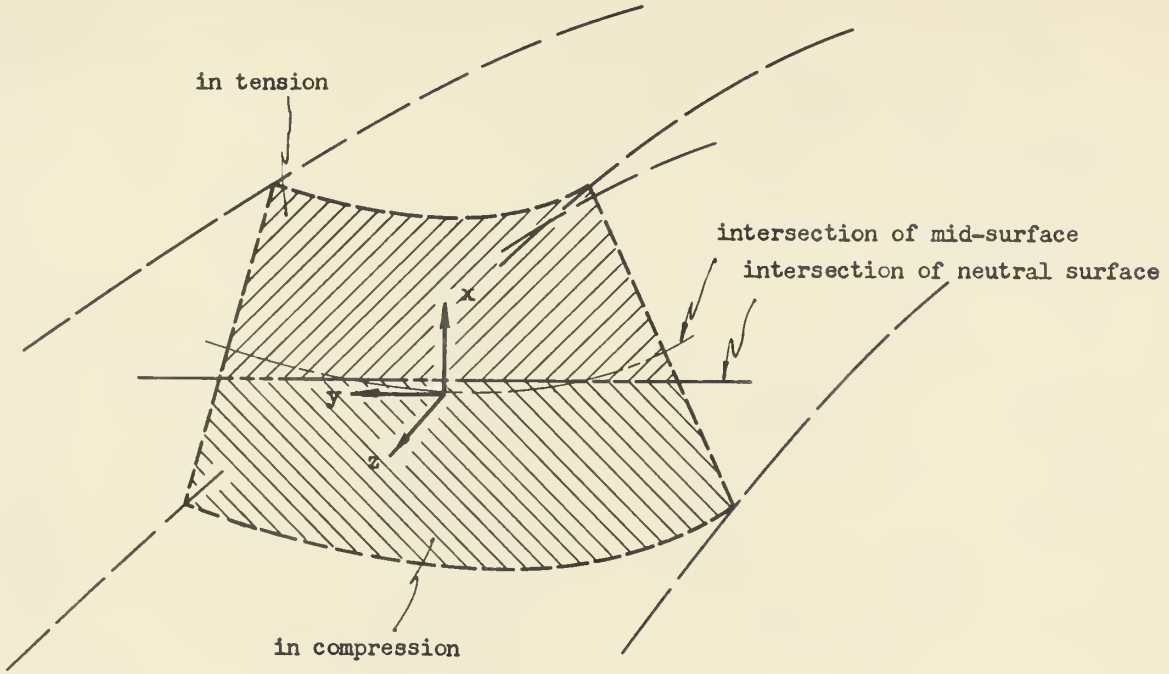

Figure 4.

Cross-section of Beam Bent in Completely Free Anti-clastic Bending Showing Anti-symmetry of σ_z.

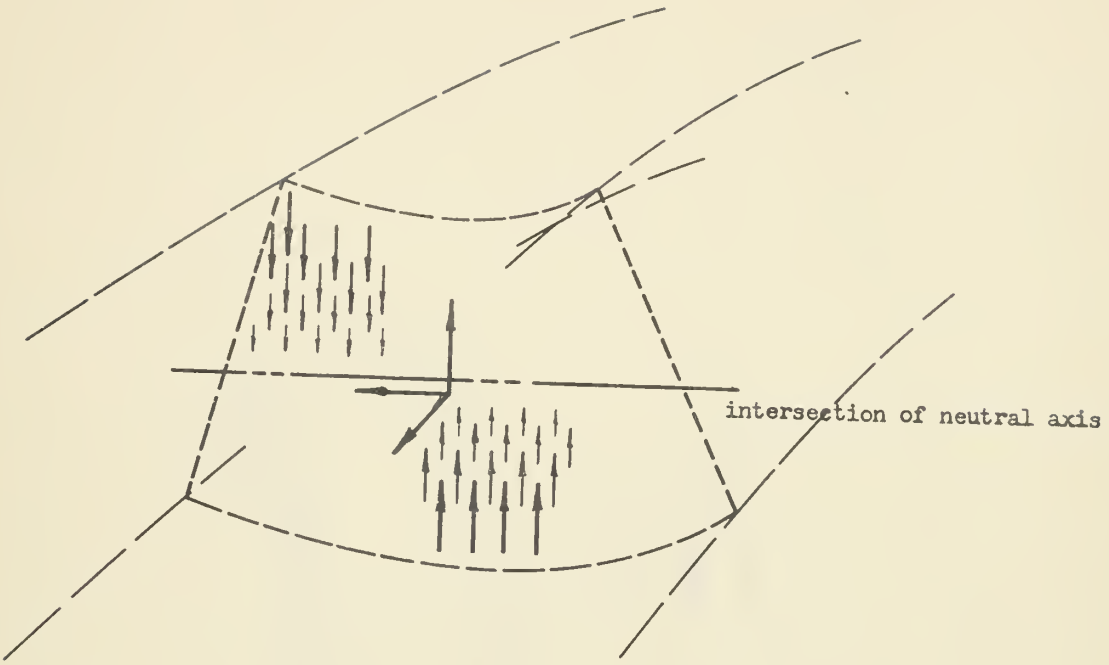

Figure 5.

Cross-section of Beam Bent in Completely Free Anti-clastic Bending Showing anti-symmetry of σ_r'.

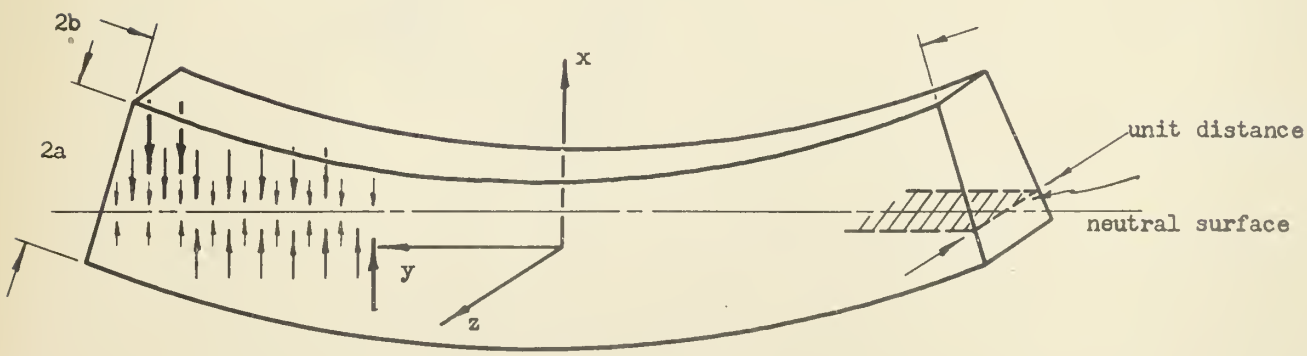

Figure 6.

Derived Beam

(From Figure 5)

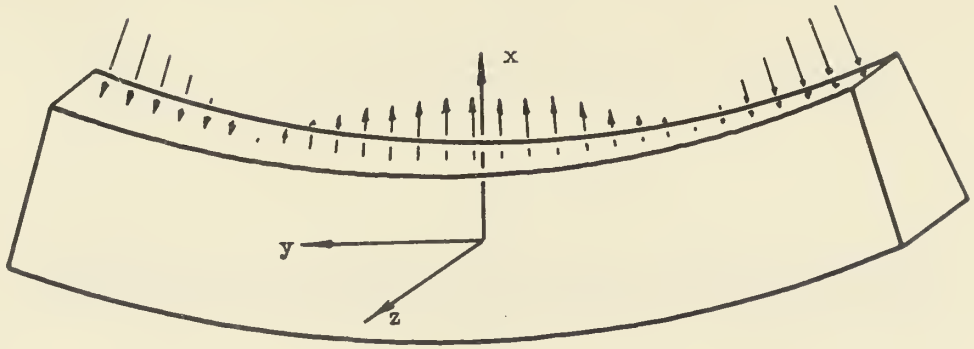

Figure 7.

Derived Beam

(From Figure 6)

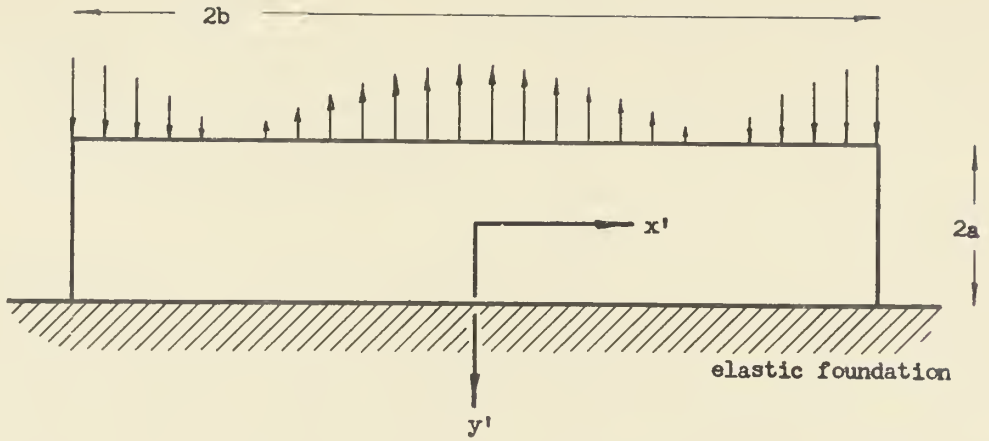

Figure 8.

Beam on an Elastic Foundation

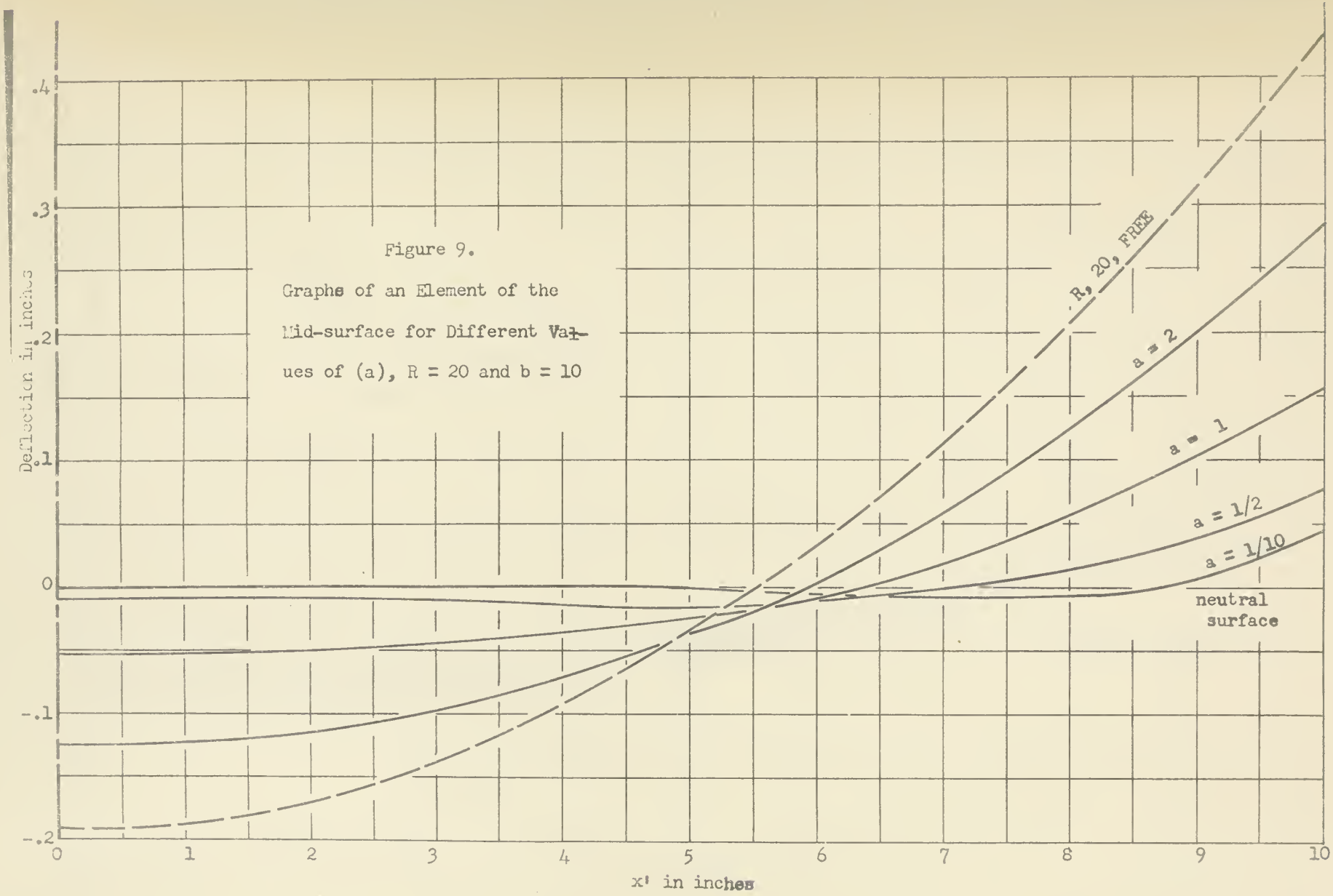

Figure 9.

Graphs of an Element of the Mid-surface for Different Values of (a), R = 20 and b = 10

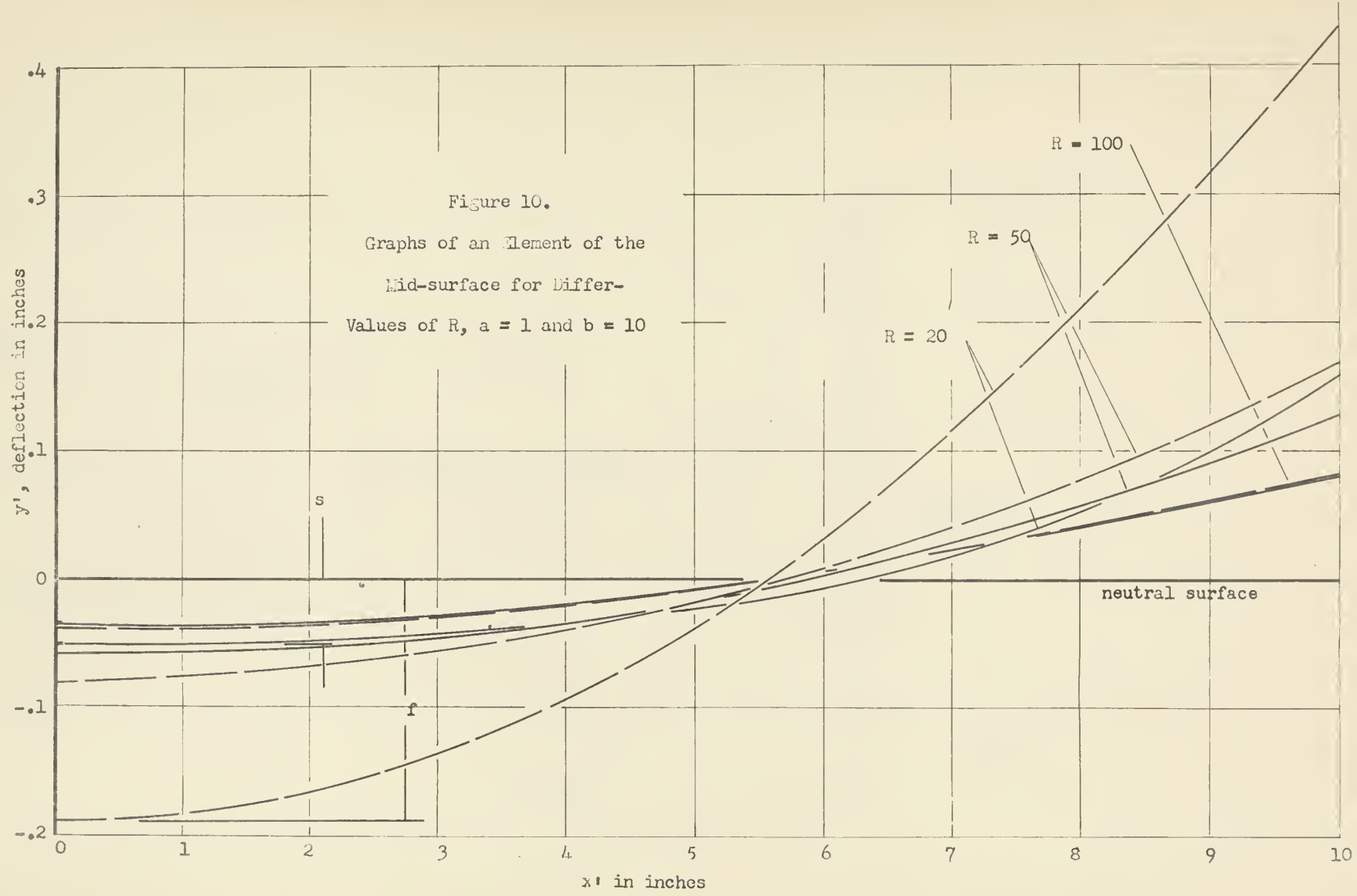
Figure 10.
Graphs of an Element of the
Mid-surface for Differ-
Values of R, a = 1 and b = 10
R = 100
R = 50
R = 20
neutral surface
s
f
y', deflection in inches
x' in inches
.4
.3
.2
.1
0
-.1
-.2
0
1
2
3
4
5
6
7
8
9
10

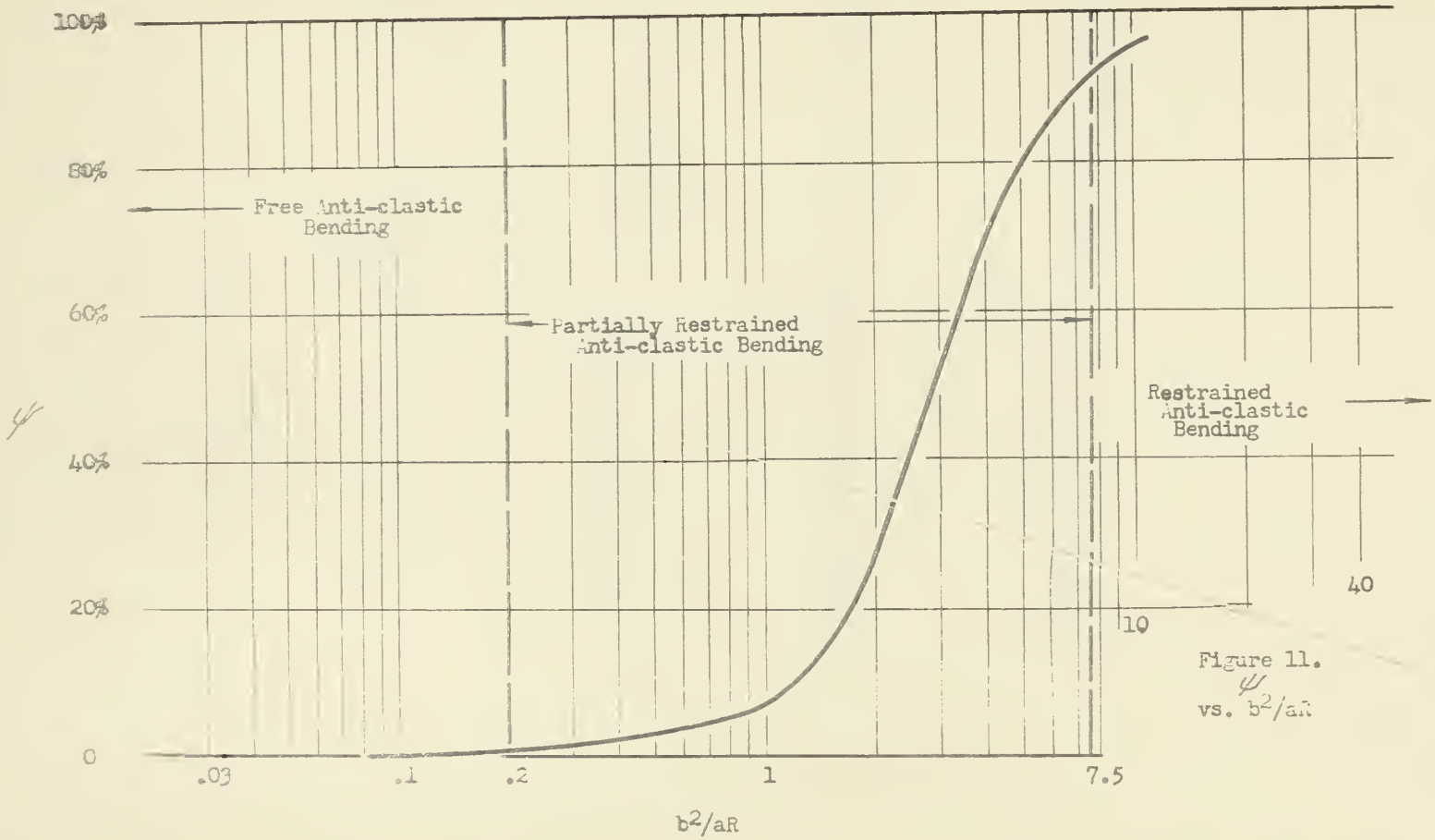

Figure 11.
ψ vs. b^2/aR

12a.

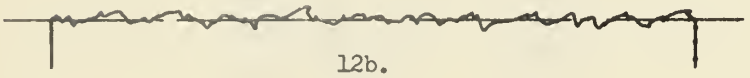

12b.

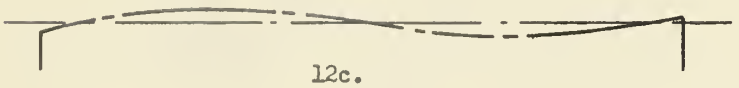

12c.

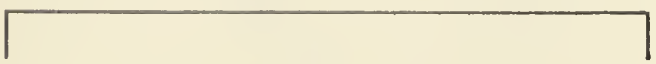

12d.

Figure 12.

"Flat" and "Smooth" Surfaces

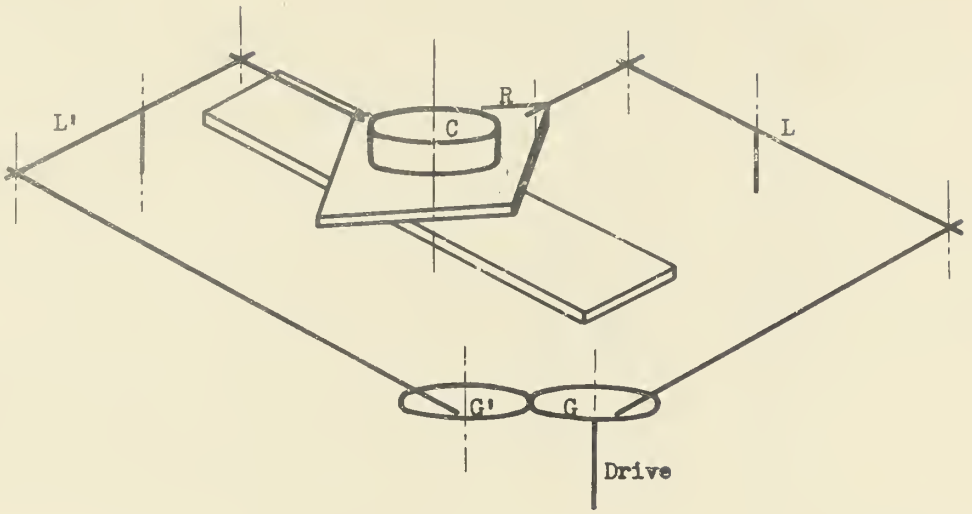

Figure 13.

Schematic of Lapping Machine

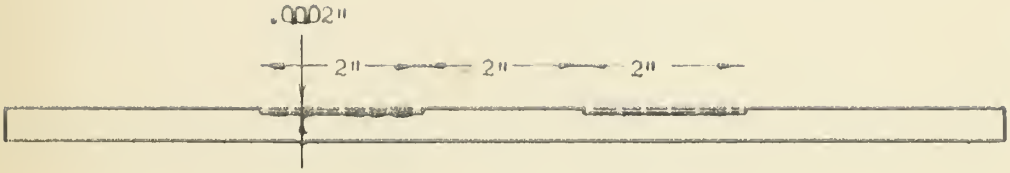

Figure 15.

Undercut Specimen

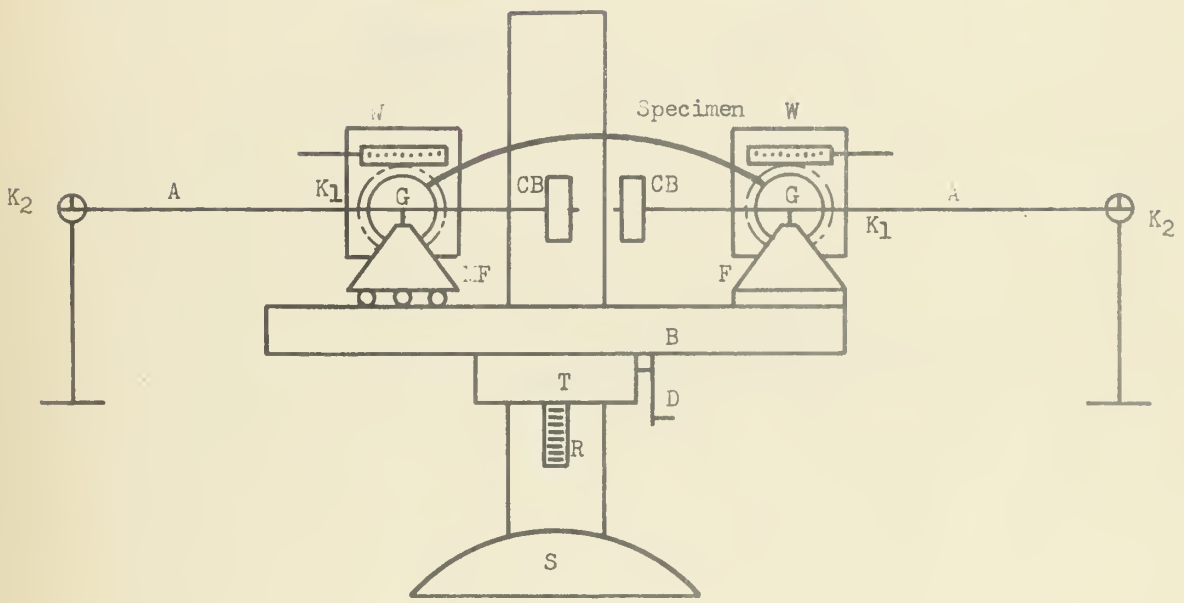

Figure 16

Proposed Bending Jig

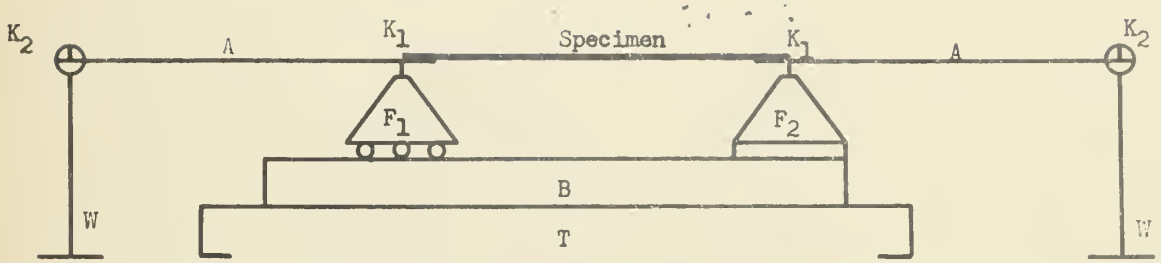

Figure 17.

Bending Jig for Electric Strain Gages

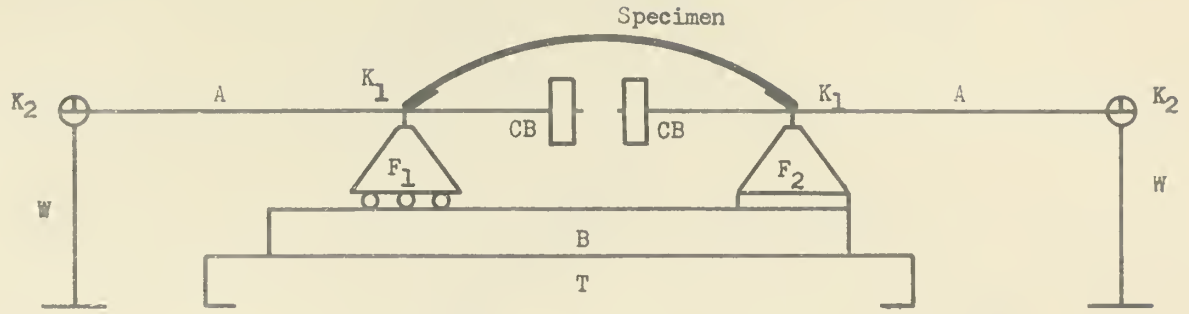

Figure 18.

Revised Bending Jig of Figure 17.

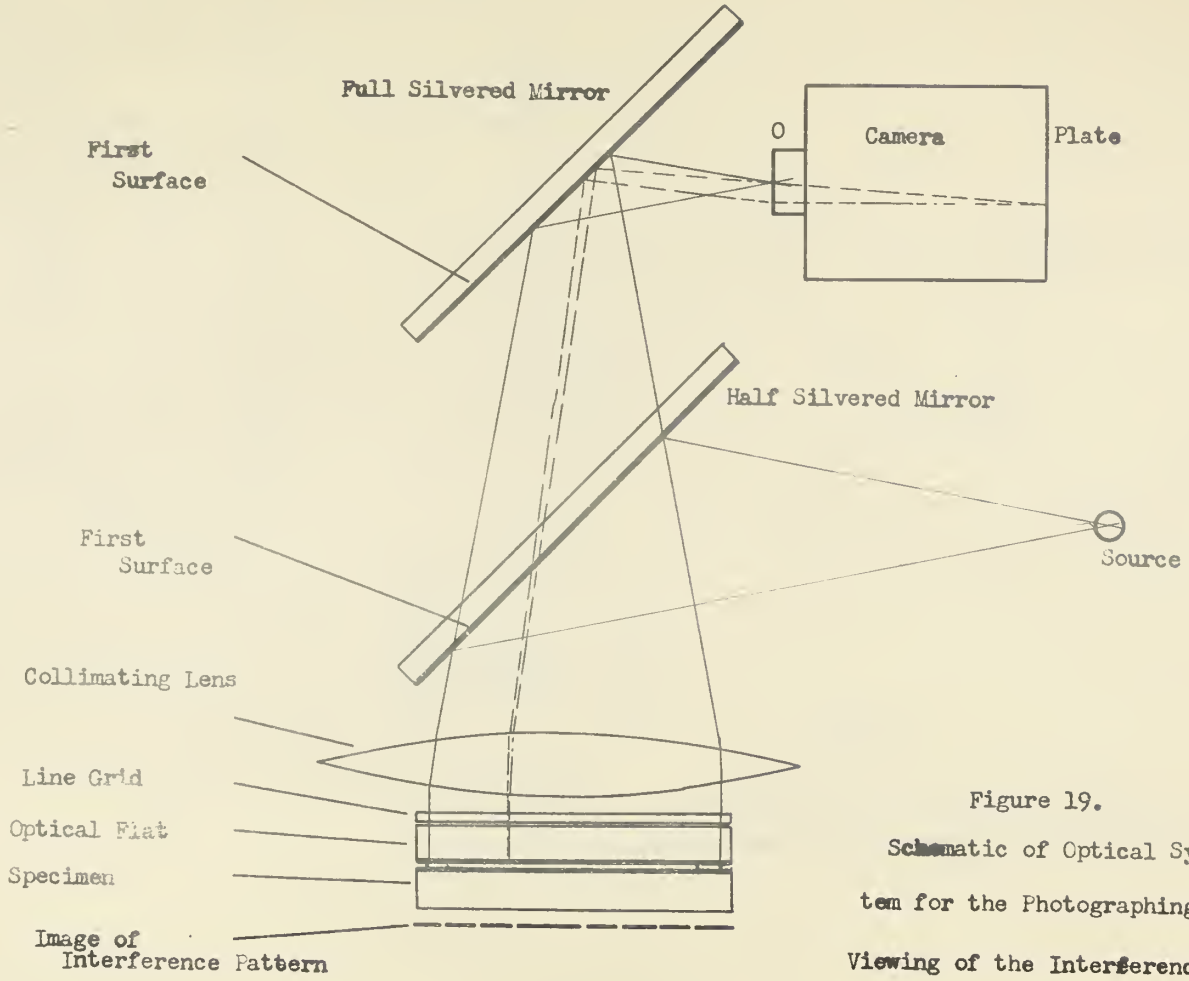

Figure 19.

Schematic of Optical System for the Photographing and Viewing of the Interference Pattern Created Between an Optical Flat and a Prismatic Bar in Pure Bending

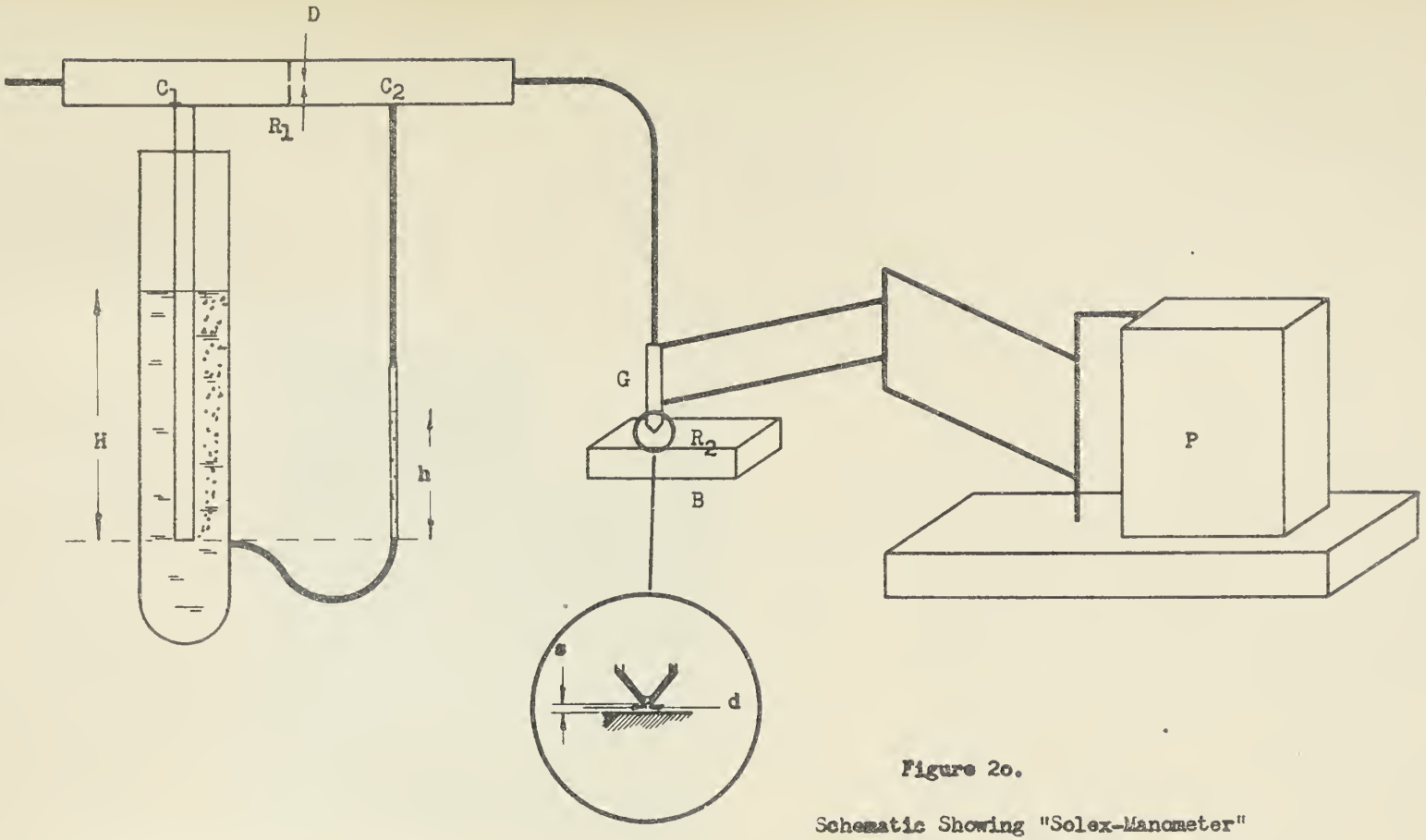

Figure 2o.

Schematic Showing "Solex-Manometer" Gage, and Pivot in Position for Testing